Rev.Adv.Mater.Sci. 25 (2010) 233-240

CHARACTERIZATION OF CREEP BEHAVIOUR AND MICROSTRUCTURE CHANGES IN PURE COPPER PROCESSED BY EQUAL-CHANNEL ANGULAR PRESSING

PART II. THE MICROSTRUCTURAL CHARACTERISTICS

I. Saxl[1,2], V. Sklenička[3], L. Ilucová[2], M. Svoboda[3], P. Král[3] and J. Dvořák[3]

[1]Faculty of Mathematics and Physics, Charles University, Sokolovská 83, CZ-186 75, Praha, Czech Republic
[2]Mathematical Institute, Academy of Sciences of the Czech Republic, Žitná 25, CZ-115 67 Praha, Czech Republic
[3]Inst. of Physics of Materials, Academy of Sciences of the Czech Republic, Žižkova 22, CZ-616 62 Brno, Czech Republic

Received: December 01, 2009

Abstract. The effect of ECAP technology with different number of passes on the structure of pure coarse grained copper is examined by means of EBSD technique. Profile and intercept counts are carried out in three mutually perpendicular planes and in several directions and the results are used to estimate (by means of stochastic geometry approaches) global 3D characteristics of multi-connected systems of grain and subgrain boundaries and grain junctions. Beside as-pressed specimens, also the specimens after annealing and after creep are examined. The relations between structural characteristics and results of creep experiments summarized in the Part I of the paper are discussed.

1. INTRODUCTION

The development of the original coarse grain and subgrain structure as the result of equal-channel angular pressing (ECAP) technology (number of passes N =1, 2, 4, 8, 12), after subsequent annealing and creep in copper is the topic of the second part of our paper. The results are compared also with the previous similar studies carried out for originally coarse grain aluminium [1-5]. The grain and subgrain structures were revealed by means of the electron backscatter diffraction (EBSD) and characterized by the unbiased estimates of the mean area intensity (density) of boundaries and subboundaries per unit volume S and by the mean length intensity (density) of triple grain and subgrain junctions per unit volume L obtained by the intercept and profile counts, respectively. They are the basic global characteristics of the material and, moreover, can be reliably estimated by the methods of stochastic geometry without any special assumptions concerning the boundary structure. The size dispersion of grains was described indirectly by the coefficients of variation of profile areas CV a.

Corresponding author: V. Sklenička, e-mail: sklen@ipm.cz

2. EXPERIMENTAL PROCEDURES

The ECAP technology used as well as the conditions of the subsequent creep were described in the first part of the paper. As-pressed specimens, specimens after annealing at 473 and 573K for 10 and 100 hours and specimens after creep testing (at the temperatures 473 and 573K at various stresses) were examined by means of scanning electron microscope (Philips SEM 505) equipped with an electron backscatter diffraction (EBSD) unit to determine the boundary disorientation distribution and the populations of high-angle grain boundaries.

Similarly as in the previous studies devoted to aluminium [1-5], at a selected place (near the specimen head in the specimens after creep) were made three mutually perpendicular planar sections denoted *XY*, *XZ* (longitudinal sections) and *YZ* (transverse section), where *X, Y*, and *Z* are the axes of a Cartesian coordinate system with *X* along the last pressing direction and *Z* perpendicular to the bottom of the channel. Four intervals of the boundary misorientation D were examined, namely subgrain boundaries with $2° \le \Delta < 5°$ and $5° \le \Delta < 10°$, transitive subboundaries $10° \le \Delta < 15°$, and, finally, conventionally defined high angle grain boundaries $\Delta \ge 15°$. Then the standard intercept count in six systematically selected directions (0^o, 30^o, 60°, 90°, 120°, 150° starting with some coordinate axis) was carried out in each section and the mean value N_L (the mean number per unit length of the test line intercepts with profile boundaries) was determined. It should be stressed, that the intercept count estimates not only the mean length of profile boundaries per unit area L_A, namely $[L_A] = (4/\pi)N_L$ (the brackets denote the unbiased estimation). If it is carried out in suitably selected section planes then the mean value N_L estimates the 3D area density S, namely $[S] = 2N_L$ (18 spatial directions were thus usually examined in each specimen). It is somewhat curious that the American Society for Testing and Materials in the *Standard methods for determining average grain size* ASTM E-112 and in particular on its contemporary web-pages states that the recommended test methods *i.e*. profile and intercept counts, deal only with determination of planar grain size, that is, with the characterization of the two-dimensional grain sections revealed by the sectioning plane. As already noted above, the mean chord length $[\mu] = 1/N_L$ is inversely proportional to the length of profile boundaries per unit area of section plane and as a global quantity it does not contain an information on individual profile sizes. The reason of this situation is that sampling of grains by section planes as well as sampling of profiles by test lines are biased by the size of grains and profiles, namely the greater objects are sectioned more frequently. Profile count is also a global quantity characterizing the sectioning of grains and subgrains by various planes; if it is independent of the section plane orientation, the structure is isotropic and if it is independent of the plane positions then the structure is homogeneous. However, under certain assumption, it has also a 3D interpretation. As already mentioned above, a useful characteristic of the grain and subgrain structure is also the multiconnected system of grain junctions. Clearly, its intersection with the section plane are profile vertices and again a relation between the mean number of such vertices per unit area P_A and L holds, namely $[L] = 2P_A$. If only triple grain junctions are encountered or at least highly prevailing and the system of profiles can be considered as a random 2D tessellation, then the mean number of vertices per profile is 2 and $[L] = 4N_A$. Summarizing these results, the intercept count estimates the mean area of boundaries and the profile count the mean length of grain junctions per unit volume. For a discussion concerning these stereological relations see *e.g.* [6,7]. Note that the model grain structure composed by space filling cubes with edge length a [μm] (hence the grain or subgrain volume is a^3 [μm^3]) has $S = 3a^{-1}$[μm^{-1}] and $L = 3a^{-2}$[μm^{-2}]. The mean chord length as measured and averaged in section planes is then 2/3[μm].

3. RESULTS

3.1. As pressed state

Selected examples of images produced by EBSD are presented in the following figures. Thus as-pressed structures of copper are shown in Fig. 1.

Note the vast diagonal profiles of subgrains after $N = 2$, 4 at $\Delta \ge 2°$ which turn out sometimes to belong to one profile only of an extensive true grain at $\Delta \ge 15°$ but frequently are also sections of true grains; typically they are observed in the *XZ* and *YZ* section planes. Note also that a diagonal orientation have also grain profiles after $N = 8$.

A typical feature of copper structure after ECAP is the presence of very small roughly spherical small precipitate-like true grains dispersed within much greater subgrain and true grain profiles. They are formed already during the first two passes and perhaps remain stable during the subsequent passes. They are also responsible for the approximately constant (60 – 70%, see Table 1) fraction of high

Table 1. Total area intensity S ($\Delta \geq 2^o$) of subgrain and grain boundaries and the proportional fractions of intensity S ($\Delta \geq 2^o$) corresponding to the chosen ranges of misorientation Δ in as-pressed specimens and as-pressed and subsequently annealed specimens corresponding to the chosen ranges of misorientation Δ.

	Intensity S [μm^{-1}] *and its fractions* (in %) *in* Δ*-ranges of*								
	as-pressed Cu				*annealed* Cu				
Δ-ranges	*N*				*N* = 2	8			
					473K	473K		573K	
	1	2	4	8	100 h	10 h	100 h	10 h	100 h
[2°,5°)	63	19	25	12	57	3	11	6	14
[5°,10°)	0	6	13	11	1	1	1	1	1
[10°,15°)	0	2	5	5	1	1	1	1	1
≥ 15°	37	73	57	72	41	95	87	92	84
S ($\Delta \geq 2°$)	0.35	2.27	3.00	3.64	0.46	0.97	0.87	0.79	0.80

Table 2. Coefficients of profile area variation CV *a* in as-pressed and in as-pressed and subsequently annealed specimens at the different values of the lower bound Δ.

	CV a in as-pressed Cu				*CV a in annealed Cu*				
$\Delta \geq$	*N*				*N* = 2	8			
					473K	473K		573K	
	1	2	4	8	100 h	10 h	100 h	10 h	100 h
2°	**8.5**	**8.5**	3.7	2.3	11.2	2.1	3.4	2.0	2.5
5°	**6.5**	**11.2**	**11.3**	**6.5**	4.7	2.0	2.9	1.9	2.4
10°	4.8	**15.6**	**13.7**	**6.7**	4.0	2.0	3.9	1.9	2.3
15°	4.3	**16.6**	**14.0**	**6.8**	3.9	2.0	3.7	1.9	2.3

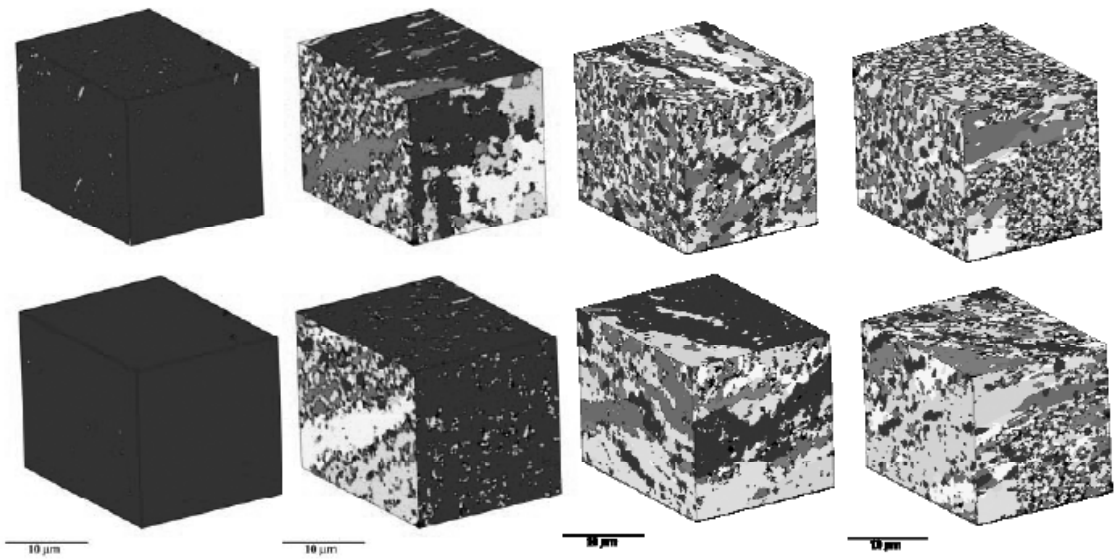

Fig. 1. EBSD images of as-pressed copper (*Z* axis is vertical, upper sides are the *XY* sections, left sided *XZ* sections and right (frontal) sides are transverse *YZ* sections), the length of the cube edge is 22 μm: $\Delta \geq 2°$ (upper row), $\Delta \geq 15°$ (lower row), $N = 1$ (left), 2 (middle), 4 (middle), 8 (right).

angle boundaries. Their mean grain volume is of the order of 1 μm^3 and their presence is responsible for the extremely high grain and subgrain size dispersion, especially at $N = 2$ and 4 (see Table 2). Consequently, in contrast to aluminium, high angle boundaries strictly prevail with the only exception at $N = 1$ and also the fraction of subboundaries with $5° \leq \Delta < 15°$ is low. The mean grain volume is of the order of 1 μm^3, but the grain size dispersion is extremely high as is shown by the values of the profile area variations (see Table 2); the values of CV *a* about 1 are usually encountered in common metallic structures.

The case of $N = 1$ is somewhat exceptional: the high angle boundaries were very scarce in two examined specimens because of the grain profile sizes exceeding the observing window. Consequently, the mean values of *S* at $N = 1$ given in Table 1 perhaps overestimate the real situation. The area intensity of the high angle boundaries *S* ($\Delta \geq 15°$) is of the order of 2 μm^{-1}**,** whereas the intensity *S* ($\Delta \geq 15°$) of the original material is approximately 0.002 μm^{-1} (the mean chord was about 1.2 mm). Consequently, the grain refinement by at least two passes is already about 10^4 times as estimated by the area intensity of high angle boundaries.

The length intensity of triple grain and subgrain junctions *L* in as-pressed specimens was not examined because its relation to boundary area is completely distorted by the presence of small isolated subgrains and grains without any junctions.

3.2. As-pressed and annealed specimens

The structural characteristics of copper annealed after $N = 2$ and $N = 8$ (at two different temperatures in this case) are presented in Fig. 2. After annealing of the $N = 2$ specimen, some small dispersed subgrains are retained and their contribution to the total boundary and subboundary area intensity is prevailing; their fraction is about 60% (see Table 1).

The situation is reversed in $N = 8$ specimens, where subboundaries play a smaller role (their fraction is only about 25% or even lower and the subboundaries with $10° \leq \Delta < 15°$ are nearly completely missing – see Table 1). The grain coarsening produced by annealing is quite considerable as demonstrated by the decrease of *S* roughly to one fourth of the value in as-pressed specimen (*S* ($\Delta \geq 15°$) is approximately 0.8 μm^{-1}). Also the grain and subggrain size dispersion is much lower as testified by the CV *a* values presented in Table 2. The length densities of triple grain and subgrain junctions *L* in annealed specimens are compared in Table 5; triple grain junctions prevail over subgrain junction.

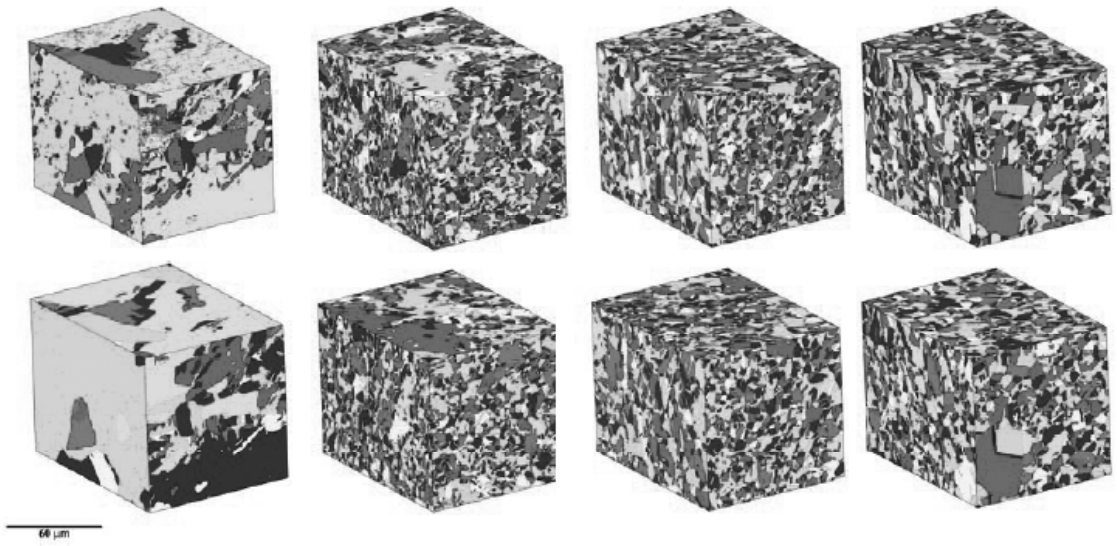

Fig. 2. *N*=2 **473K/100h** *N*=8 **473K/100h** **573K/10h** **573K/10h**
EBSD images of as-pressed ($N = 2, 8$) copper annealed at two different temperatures: D i 2° (upper row), $\Delta \geq 15°$ (lower row).

Table 3. Total area intensity S ($\Delta \geq 2°$) of subgrain and grain boundaries and the proportional fractions of intensity S ($\Delta \geq 2°$) corresponding to the chosen ranges of misorientation after creep at 473K, 80 MPa for different numbers of passes N.

	Intensity S [mm^{-1}] after creep and its fractions (in %) in Δ-ranges			
Δ-ranges	1	2	4	8
[2° 5°) 39	22	21	13	
[5° 10°) 13	2	3	0	
[10° 15°)	5	3	0	0
≥15° 43	73	76	87	
S ($\Delta \geq 2°$)	0.46	0.25	0.58	0.46

Table 4. Coefficients of profile area variation CV *a* after creep at 473K, 80 MPa for different numbers of passes N.

	CV a after creep			
$\Delta \geq$	1	2	4	8
2°	9.3	6.2	4.1	4.1
5°	7.2	4.5	3.7	3.2
10°	4.9	4.3	4.2	3.3
15°	4.1	4.7	4.2	3.2

3.3. As-pressed, shortly annealed specimens after creep

Finally, we shall consider the considerably different structures after creep, which are shown in Fig. 3, whereas the quantitative structural results are summarized in Tables 3, 4, and 5. The annealing times at different stresses and temperatures were substantially diverse, namely several hundred of hours at N = 1, 2 and stress 80 MPa at 473K and between approx. 70 and 140 hours in the remaining cases.

The substantial grain coarsening came up (very roughly about 10 times in the mean grain width at 473K; see again Tables 1 and 3). However, from the qualitative point of view (subgrain and grain shapes, profile dispersion), the structures developed after the number of passes N = 2, 4 and 8 are similar. The previously observed structural features, in particular particle-like subgrains and grains freely dispersed within larger grains can be again observed. Twins are rather frequent and were not observed in the as-pressed and annealed specimens. Table 1 again confirms the low share of subboundaries with $5° \leq \Delta < 15°$.

The length intensities of triple grain and subgrain junctions L after creep (Table 5) show that triple grain and subgrain junctions are less dense than after annealing and, moreover, compared in Table 5; triple subgrain junctions slightly prevail over grain junction.

Further, there is not a systematic dependence of CV *a* after creep on the number of passes but the dispersion of grain profiles is slightly more homogeneous than that one of subgrains, in particular at $N \geq 8$ at 473K.

The comparison of these results with those ones obtained in aluminium shows, that the dispersion of grain and subgrain profiles in copper in all examined situations is nearly twice as high (as measured by the values of CV *a*).

Table 5. Total length intensity L ($\Delta \geq 2°$) of triple subgrain and grain junctions boundaries and its fractions (in %) corresponding to the chosen ranges of misorientation after annealing of as-pressed specimens and after their creep at 473K, 80 MPa.

	Intensity L[mm^{-1}] and its fractions (in %) in Δ-ranges of annealed Cu of Cu after creep at 473K									
Δ-ranges	N = 2	8				N				
	473K	*473K*	*573K*							
	100 h	10 h	100 h	10 h	100 h	1	2	4	8	12
[2° 5°)	52	18	25	18	30	74	64	47	39	54
[5° 10°)	35	0	0	0	0	7	4	5	5	2
[10° 15°)	0	6	0	0	0	2	0	4	3	1
≥ 15°	13	76	75	82	70	17	32	44	53	43
L ($\Delta \geq 2°$)	0.25	0.68	0.53	0.44	0.40	0.18	0.10	0.30	0.23	0.18

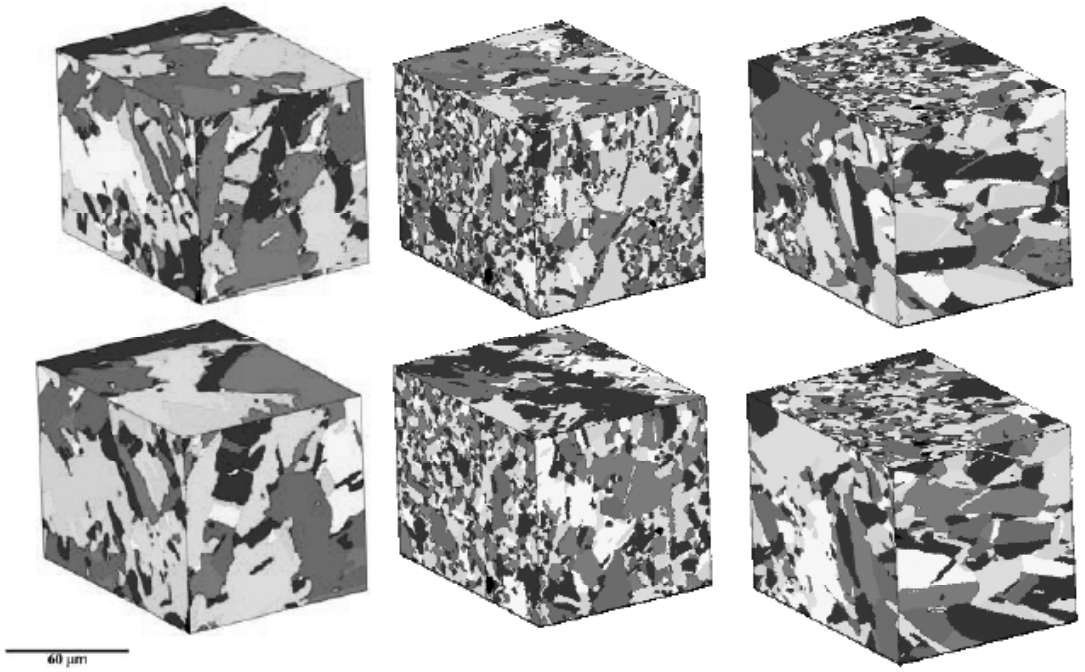

Fig. 3. EBSD images of of copper specimens after annealing during the creep tests at 473K and 80 MPa: $\Delta \geq 2°$ (upper row) and $\Delta \geq 15°$ (lower row), $N = 1$ (left), 4 (middle), 12 (right).

The results concerning intensities S in aluminium and copper for the fractions corresponding to high angle boundaries with $\Delta \geq 15°$ are compared in Fig. 5. Whereas the growth of these fractions with the repeating number of passes is quite distinct in aluminium, such a behavior cannot be proved for copper and the differences in S at individual values of N reflect rather a great scatter of results than some reasonable dependence (in particular at $N = 1$).

The estimated values of the coefficients of variation CV a describing the profile size dispersion (*i. e.* local homogeneity of subgrain and grain structure) on the area of observation window (475 μm^2 in as-pressed specimens and about 12 400 μm^2 in the remaining cases) are presented in Tables 2 and 4. Extremely high values are found in the as-pressed specimens (note that CV a in relatively homogeneous grain systems should not exceed the value of 1) at all values of the lower bound of misorientation D and they systematically increase with growing Δ, perhaps as a consequence of vanishing small subgrains (the results obtained at $N = 1$ are not

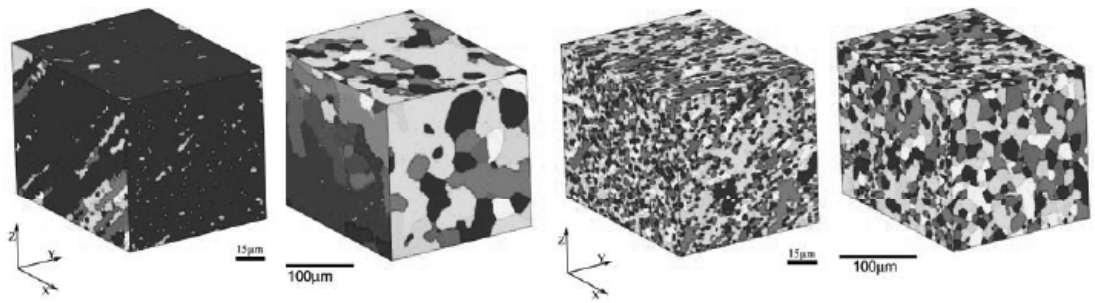

Fig. 4. ***N* = 2** ***N* = 12**

EBSD images of aluminium grains ($N = 2, 12$; $\Delta \geq 15°$) in as-pressed specimens (left) and after the creep tests at 473K and 80 MPa (right).

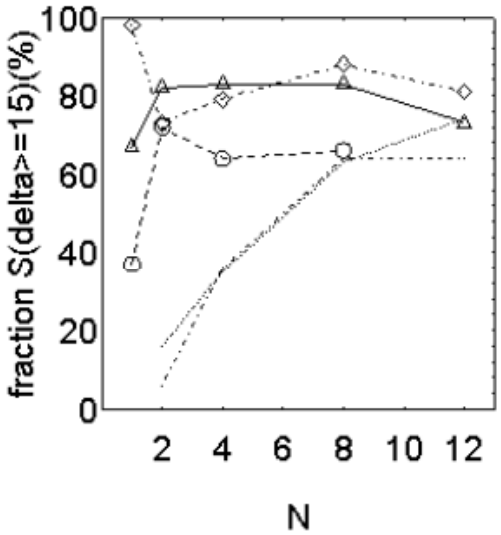

Fig. 5. Fraction of true high angle boundaries ($\Delta \geq 15°$) for as-pressed copper (circles) and after creep at 473K (80 MPa, triangles) and 573K (50 MPa, squares) as compared with aluminium (as-pressed, dotted line) and after creep (473K and 20 MPa, dash-and-dot).

reliable because the observing window is too small). On the other hand, both the annealing times at both the temperatures produce similar grain profile dispersions with CV *a* approximately equal to 2.

4. CONCLUDING DISCUSSION

Perhaps the most interesting feature of copper subgrain and grain structures after ECAP is the deficit of small angle boundaries with the misorientation from the interval $5° \leq \Delta < 15°$. They are nearly completely missing in the annealed as-pressed specimens (see Table 1; their area fraction does not exceed 2%) and only rarely exceed 10%. The contribution of subboundaries with $\Delta < 5°$ never attain the 30-percent level, the grain structures look unstable and are inhomogeneous (with CV *a* values between 3.5 and 5.8 even after 12 passes and creep at 573K).

The completely different behaviour was observed in aluminium, in which the proportion of high angle boundaries grew continually with the increasing number of passes in as-pressed specimens as well as after their annealing during creep tests, see Fig. 5. Relatively homogeneous structures (with CV $a \approx 2$) are formed after higher number of passes and creep The contribution of subgrains with medium boundary misorientation $5° \leq \Delta < 15°$ systematically exceeded that one of low angle ($\Delta < 5°$) subboundaries at $N \geq 4$ (see [2,4]). Even when small subgrains and grains scattered within larger grains and subgrains were also observed in aluminium, they were less numerous and less stable than in copper and rather exceptional after creep.

A detailed discussion concerning the effect of ECAP pressing on the creep properties is in [5,7] and it is only shortly summarized here. The lack of high-angle boundaries can be the reason of high creep resistance after the first pass. The gradual development of such boundaries during subsequent passes makes the dislocation movement easier, the creep rate increases and approximately constant ultimate elongation is attained in a shorter time.

However, such an explanation is unacceptable in the case of copper, where the high angle boundaries are present in reasonable amount even at low number of passes. Nevertheless, certain grain growth also proceeds in copper; it seems that the number of small particle-like grains decreases and at least certain of them transform into larger grains thus promoting the creep by the dislocation motion. The difference in the homological temperatures of copper and aluminium can also influence the creep behavior as well as the structure development. In any case, it seems that a more detailed examination of copper grain structures after ECAP and creep is necessary in order to explain reliably their creep properties.

ACKNOWLEDGEMENTS

The authors acknowledge the financial support for this work provided by the GA ČR (grant 201/06/0302), by the grant MSM 0021620839 and by the Academy of Sciences of the Czech Republic, Institutional Research Plans No. AV0Z10190503 and AV0Z20410507.

REFERENCES

[1] L. Ilucová, I. Saxl, M. Svoboda, V. Sklenička and P. Král // *Image Analysis and Stereology* **26** (2007) 37.

[2] I. Saxl, L. Ilucová, M. Svoboda, V. Sklenička, V.I. Betekhtin, A.G. Kadomtsev and P. Král // *Mater. Sci. Forum* **567-568** (2008) 193.

[3] I. Saxl, V. Sklenička, L. Ilucová, M. Svoboda and P. Král // *Mater. Sci. Forum* **561-565** (2007) 813.

[4] I. Saxl, V. Sklenička, L. Ilucová, M. Svoboda, J. Dvořák and P. Král // *Mater. Sci. Eng. A* **503** (2009) 82.
[5] V. Sklenička, J. Dvořák, P. Král, M. Svoboda and I. Saxl // *Int. J. Mat. Res.* **100** (2009) 762.
[6] D. Stoyan, W.S. Kendall and J. Mecke, *Stochastic Geometry and Its Applications* (Wiley & Sons, Chichester, 1995).
[7] I. Saxl and V. Sklenička // *Mater. Sci. Forum* **604-605** (2009) 403.